

# Contribution of Residues in Second Transmembrane Domain of ASIC1a Protein to Ion Selectivity\*

Received for publication, December 2, 2011, and in revised form, February 13, 2012. Published, JBC Papers in Press, February 27, 2012, DOI 10.1074/jbc.M111.329284

Marcelo D. Carattino<sup>‡§1</sup> and Margaret C. Della Vecchia<sup>‡</sup>

From the Departments of <sup>‡</sup>Medicine and <sup>§</sup>Cell Biology and Physiology, University of Pittsburgh, Pittsburgh, Pennsylvania 15261

**Background:** The mechanisms of ion selectivity and permeation of acid-sensing ion channels are not solved.

**Results:** Substitutions at selected sites altered cation discrimination.

**Conclusion:** Ion selectivity is achieved by discrimination of ions on the basis of size and by selective coordination at restricted sites in the pore of ASIC1a.

**Significance:** Elucidating the mechanisms of ion permeation and selectivity of ASIC1a is important to understand its function and physiological role.

Acid-sensing ion channels (ASICs) are proton-gated cation-selective channels expressed in the peripheral and central nervous systems. The ion permeation pathway of ASIC1a is defined by residues 426–450 in the second transmembrane (TM2) segment. The gate, formed by the intersection of the TM2 segments, localizes near the extracellular boundary of the plasma membrane. We explored the contribution to ion permeation and selectivity of residues in the TM2 segment of ASIC1a. Studies of accessibility with positively charged methanethiosulfonate reagents suggest that the permeation pathway in the open state constricts below the gate, restricting the passage to large ions. Substitution of residues in the intracellular vestibule at positions 437, 438, 443, or 446 significantly increased the permeability to  $K^+$  versus  $Na^+$ . ASIC1a shows a selectivity sequence for alkali metals of  $Na^+ > Li^+ > K^+ \gg Rb^+ > Cs^+$ . Alanine and cysteine substitutions at position 438 increased, to different extents, the relative permeability to  $Li^+$ ,  $K^+$ ,  $Rb^+$ , and  $Cs^+$ . For these mutants, ion permeation was not a function of the diameter of the nonhydrated ion, suggesting that Gly-438 encompasses an ion coordination site that is essential for ion selectivity. M437C and A443C mutants showed slightly increased permeability to  $K^+$ ,  $Rb^+$ , and  $Cs^+$ , suggesting that substitutions at these positions influence ion discrimination by altering molecular sieving. Our results indicate that ion selectivity is accomplished by the contribution of multiple sites in the pore of ASIC1a.

The epithelial sodium channel/degnerin (ENaC/DEG)<sup>2</sup> family comprises cation-selective channels with diverse functions in animal physiology (1). The molecular bases of ion per-

meation and discrimination of these channels are poorly understood. ENaC/DEG channels are organized as homo- or heterotrimers. Each subunit has two transmembrane (TM) segments, a large extracellular region, and intracellular N and C termini. Despite the fact that residues in segments forming the permeation pathway are particularly well conserved among ENaC/DEG subunits, functional studies revealed dramatic differences in terms of ion selectivity between family members. Acid-sensing ion channels (ASICs) are proton-gated members of this family with moderate selectivity toward alkali metals (2–5). These channels are expressed in the central and peripheral nervous systems where they contribute to nociception, mechanosensation, fear-related behavior, and seizure termination (6–8). In contrast, ENaCs are particularly selective for  $Na^+$  over  $K^+$  with a permeability ratio  $>100$ , therefore constituting a selective pathway for  $Na^+$  absorption in epithelia (1, 9, 10).

Structural features that allow selective permeation of ions have been defined for tetrameric channels including  $K^+$ ,  $Ca^{2+}$ ,  $Na^+$ , and cyclic nucleotide-gated channels (11).  $K^+$  channels contain a conserved signature sequence TVGYG in the S5-S6 linker that forms the coordination sites for cations. Four sites for dehydrated  $K^+$  ion coordination are defined by the backbone carbonyl groups of TVGYG residues, along with the hydroxyl oxygen of the Thr residue (12). Tetrameric  $Na^+$  and  $Ca^{2+}$  channels have modest and high negatively charged residues in the pore, respectively, that comprise the sites for cation coordination (11). The resolved structure of chicken ASIC1 (cASIC1) in the desensitized-like state shows that the pore has an asymmetric hourglass-like shape with the intracellular and extracellular vestibules defined by the intersection of the TM2 helices (13). ENaC/DEG channels do not have negatively charged residues in the TM2 segments that could serve as coordination sites for cations. The permeation pathway of these channels is formed for the most part by nonpolar amino acids. Mutagenesis studies on ENaC ascertained the contribution of residues in the TM2 helices to ion permeation and discrimination and amiloride binding (14–20). The high  $Na^+$  selectivity of ENaC has been ascribed to a conserved (G/S)XS tract in the TM2 segment (15–19). Substitutions of the third position dramatically increase the permeability to  $K^+$  of ENaC, without a

\* This work was supported, in whole or in part, by National Institutes of Health Grant R01 DK084060-02 (to M. D. C.).

<sup>1</sup> To whom correspondence should be addressed: S828 Scaife Hall, 3550 Terrace St., Pittsburgh, PA 15261. Tel.: 412-624-5437; Fax: 412-648-9166; E-mail: mdc4@pitt.edu.

<sup>2</sup> The abbreviations used are: ENaC, epithelial sodium channel; DEG, degnerin; ASIC, acid-sensing ion channel; ASIC1a, acid-sensing ion channel 1a; cASIC1, chicken ASIC1; mASIC1a, mouse ASIC1a; TM, transmembrane; MTS, methanethiosulfonate; MTSET, [2-(trimethylammonium)ethyl] methanethiosulfonate bromide; MTSEA, [2-aminoethyl] methanethiosulfonate hydrobromide.

## ASIC1a Permeation Pathway

noticeable effect on  $\text{Li}^+$  permeability. These studies suggested that ENaC discriminates on the basis of the nonhydrated diameter of the permeating cation and the energy of dehydration (18). Although the selectivity toward alkali metals of ENaCs and ASICs differs considerably, residues in the (G/S)XS tract are mostly conserved. Moreover, ENaCs bearing a  $\gamma$ S541G mutation, which resembles a Gly-X-Ser tract as present in ASIC1a, remain impermeable to  $\text{K}^+$ . Furthermore, ASIC1a is slightly more permeable to  $\text{Na}^+$  than  $\text{Li}^+$ , which cannot be explained with a model that discriminates ions on the basis of the size of their nonhydrated diameter. Overall, these facts suggest that additional residues in the TM2 segment of ASIC1a contribute to cation selectivity. Here we explore the role of residues in the TM2 segment of ASIC1a to ion permeation and selectivity.

### EXPERIMENTAL PROCEDURES

**Molecular Biology and Oocyte Expression**—Constructs were generated in a mouse ASIC1a (mASIC1a) template bearing a C70L mutation, as described previously (21). Where indicated, constructs contained a C-terminal hemagglutinin (HA) epitope tag. Site-directed mutagenesis was performed with QuikChange XL (Agilent Technologies, Santa Clara, CA) according to the manufacturer's instructions. Mutations were confirmed by direct sequencing. cRNAs were transcribed using mMESSAGE mMACHINE SP6 (Applied Biosystems, Carlsbad, CA). Oocyte stages 5–6 were isolated from adult female *Xenopus laevis* (Nasco, Plant City, FL) using a protocol approved by the University of Pittsburgh Institutional Animal Care and Use Committee. Oocytes were injected with 0.1–6 ng of cRNA encoding ASIC1a mutants and were maintained at 18 °C in modified Barth's solution containing (in mM) 88 NaCl, 1 KCl, 2.4  $\text{NaHCO}_3$ , 15 HEPES, 0.3  $\text{Ca}(\text{NO}_3)_2$ , 0.41  $\text{CaCl}_2$ , 0.82  $\text{MgSO}_4$ , 10  $\mu\text{g}/\text{ml}$  sodium penicillin, 10  $\mu\text{g}/\text{ml}$  streptomycin sulfate, 100  $\mu\text{g}/\text{ml}$  gentamycin sulfate, pH 7.4.

**Distance of  $\text{C}\alpha$  Atoms to the Long Axis of the Pore**—cASIC1 subunits (Protein Data Bank (PDB) code 3HGC) are symmetrically arranged along the long axis of the molecule. Consequently, the distances of identical atoms from different subunits in the same spatial plane to the center of the molecule are equivalent. Similarly, the distances between identical atoms in neighboring subunits are also the same. Therefore, an equilateral triangle is defined by connecting  $\text{C}\alpha$  from equivalent residues in each of the three subunits. The radius of a circumscribed circle in an equilateral triangle is defined as  $a/\sqrt{3}$ , where  $a$  is the distance between two  $\text{C}\alpha$  atoms. The radius of this circumscribed circle equals the distance of the  $\text{C}\alpha$  to the center of the pore.

**Electrophysiology**—Two-electrode voltage clamp was performed with a TEV-200A amplifier (Dagan Corp., Minneapolis, MN), as described previously (21). Experiments were performed 24–72 h after injection at room temperature (20–25 °C). Oocytes were mounted in an oocyte perfusion chamber with a volume of  $\sim 20 \mu\text{l}$  (AutoMate Scientific, Berkeley, CA) and were impaled with glass electrodes filled with 3 M KCl. The resistance of the electrodes was less than 2 megaohms in the recording solutions. Oocytes were continuously clamped at a holding potential of  $-60 \text{ mV}$ . Data were captured with an Axon Digidata 1440A acquisition system and analyzed with pClamp

10 (Molecular Devices, Sunnyvale, CA). Studies of permeability were carried out with solutions containing (in mM) 110 of the chloride salts of the indicated alkali metal, 1  $\text{CaCl}_2$ , and 10 HEPES (or MES for solutions of pH 5.0). pH was adjusted with a hydroxide of the main permeating cation in the solution.

ASIC1a tachyphylaxis refers to a reduction in the magnitude of the proton-gated current observed after successive acid stimulations (22). To minimize this phenomenon in the studies of selectivity, channels were subjected to only two cycles of activation. Consequently, data sets for each mutant were normalized for the current decay observed when channels were exposed to two consecutive cycles of activation in solutions containing  $\text{Na}^+$  as the main permeable cation.

**Accessibility to MTS Reagents**—Oocytes expressing ASIC1a bearing Cys mutations were mounted in a recording chamber and perfused with a solution containing (in mM) 110 NaCl, 2 KCl, 1  $\text{CaCl}_2$ , 10 HEPES, pH 7.4. Proton-gated currents were elicited with acidic solutions buffered with MES. Oocytes were treated with solutions containing methanethiosulfonate (MTS) reagents at pH 6.5, *i.e.* channels in a conductive state, or 7.4, *i.e.* channels in the resting state. The reactivity of the MTS reagents toward the thiolate anion is preferred to that of the protonated form of the thiol group. Consequently, channels were treated with 3 mM or 300  $\mu\text{M}$  MTSEA at pH 6.5 and 7.4, respectively. MTS reagents were directly dissolved in the recording solutions buffered at pH 7.4 or 6.5 and used within 15 or 30 min of preparation, respectively.

**Data and Statistical Analysis**—Data are expressed as means  $\pm$  S.E. ( $n$ ), where  $n$  equals the number of independent experiments analyzed. A  $p$  value of less than 0.05 was considered statistically significant.

### RESULTS

The structural bases for ion permeation and selectivity of ENaC/DEG channels are largely unresolved. Two atomic structures of cASIC1 in the desensitized-like state are currently available in the PDB: 2QTS and 3HGC. Although both structures show a similar architecture of the extracellular region, the organization of the TM segments presents notable differences (13, 23). 2QTS was resolved from proteins lacking the N and C termini, whereas 3HGC was resolved from proteins (ASIC1mfc) including the intracellular N terminus and a short segment of the C terminus. The ASIC1mfc construct, when expressed in a heterologous expression system, generates proton-gated currents with similar sodium selectivity to wild type (full-length) cASIC1 (13). The transmembrane helices are positioned symmetrically around the long axis of the pore in 3HGC. The gate, defined by the intersection of the TM2 helices, localizes near the extracellular boundary of the plasma membrane. Asp-433, in this atomic structure, outlines the bottom of the extracellular vestibule (Fig. 1). In contrast, the pore of 2QTS presents a breakdown in the molecular three-fold axis of symmetry with a desensitization gate that localizes near the intracellular boundary of the membrane (23). Fig. 1 shows the alignment of residues in the predicted TM2 helices of ENaC subunits, ASIC1a, and brain-liver-intestine  $\text{Na}^+$  channel (BLI-NaC). Residues in the TM2 segment are well conserved along

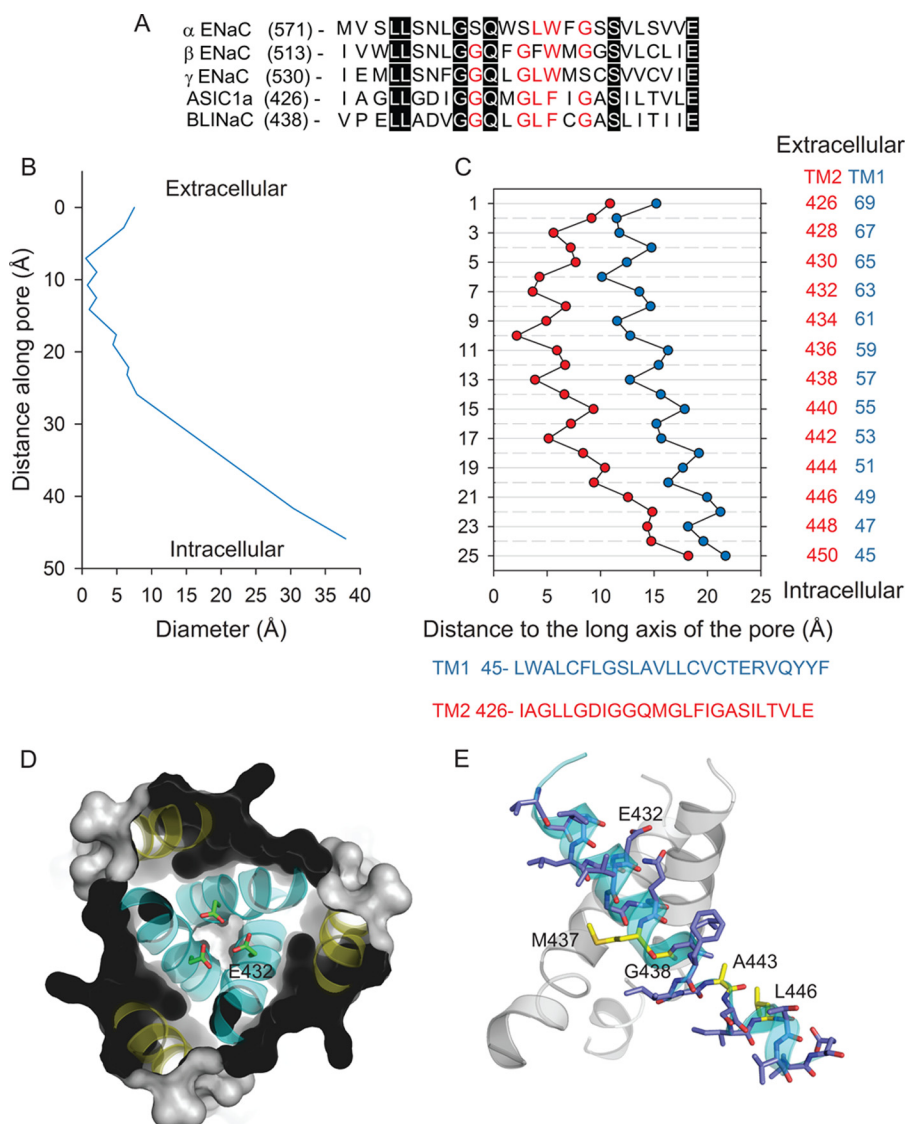


**FIGURE 1. Architecture of the pore of ASIC1.** *A*, alignment of the TM2 segments of the ENaC subunits and mASIC1a and brain-liver-intestine Na<sup>+</sup> channel (BLINaC) subunits (GenBank™ numbers NP\_035454, NP\_035455, NP\_035456, NP\_033727, and NM\_021370). Identical residues are highlighted in *black* with *white* lettering, whereas conserved residues are indicated in *red* lettering. *B*, pore diameter as a function of the longitudinal distance along the pore of cASIC1 (PDB code: 3HGC). Pore dimensions were estimated with MolAxis software. *C*, geometrical arrangement of residues along the pore of cASIC1. Distances of C $\alpha$  of residues in the TM1 and TM2 segments to the long axis of the pore of cASIC1 in the desensitized state (PDB code: 3HGC). The numbering of residues corresponds to mASIC1a. cASIC1 and mASIC1a share 72 and 96% amino acid identity in the TM1 and TM2 segments, respectively. *D*, extracellular view of the pore of cASIC1 (PDB code: 3HGC). Asp-432 (mASIC1a) constitutes the base of the extracellular vestibule. *E*, key residues identified in this study that affect ion selectivity. Numbering of residues corresponds to mASIC1a.

ENaC/DEG subunits, suggesting similar pore architecture for members of this family.

**Ion Permeation**—ASIC1a resides at least in three states, resting, open, and desensitized. Extracellular acidification triggers the transition of the channel from the closed to the open state, which then transitions to the desensitized state. These channels desensitize over a narrow range of pH. At pH values above 7.4, ASIC1a exists in the closed state, whereas at pH values below 7.2, it resides in the desensitized state (21, 24). To define structural changes associated with pore opening, we explored the reactivity of MTSET with channels bearing single Cys mutations in the tract 426–438 at pH 6.5, *i.e.* channels in a conductive state. MTSET is a membrane-impermeable reagent bearing a positively charged trimethylammonium group with a molecular diameter of  $\sim 5.8$  Å. We previously found that channels

bearing Cys substitutions at positions 426, 427, or 428 are modified by extracellular MTSET at pH 7.0, *i.e.* channels in the desensitized state, and 7.4, *i.e.* channels in the resting state (24). Fig. 2A shows a representative recording obtained from an oocyte expressing A427C channels modified by MTSET at pH 6.5, *i.e.* channels in the open state. MTSET treatment changed the magnitude of the peak current and the steady-state desensitization of this mutant. The effect on steady-state desensitization was partially reversed upon MTSET washout. This suggests that at pH 6.5, MTSET binds to the pore of modified channels, preventing closure of the permeation pathway. The relative response represents the ratio of the peak current evoked by extracellular acidification after MTSET treatment to the peak current evoked by extracellular acidification before MTSET treatment. Channels bearing single Cys substitutions

## ASIC1a Permeation Pathway

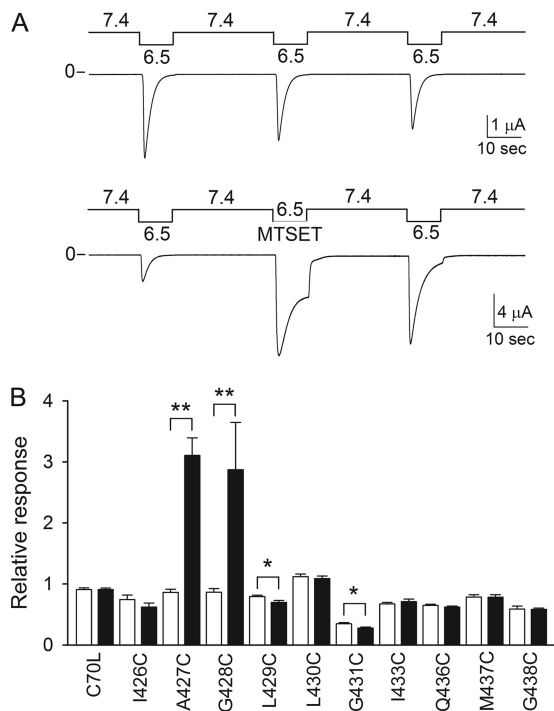


**FIGURE 2. Chemical modification by MTSET of residues in TM2 segment.** *A*, representative recording of proton-activated currents obtained from oocytes expressing A427C channels treated with MTSET (1 mM) at pH 6.5, *i.e.* channels in a conductive state. Untreated oocytes expressing A427C channels served as controls. *B*, reactivity toward MTSET of residues in the pore of ASIC1a. M437C and G438C have a C-terminal HA epitope tag. *Closed* and *open bars*, relative response to extracellular acidification of oocytes expressing ASIC1a mutants treated with MTSET (*closed bars*) and controls (*open bars*). Whole-cell currents were elicited by a change in extracellular pH from 7.4 to 6.5. The peak current evoked by extracellular acidification after MTSET treatment (or control) was normalized to the peak current evoked by extracellular acidification before treatment. Statistically significant differences are indicated as \*,  $p < 0.05$  and \*\*,  $p < 0.001$  ( $n = 5-14$ ) (Kruskal-Wallis test followed by Dunn's multiple comparisons test).

at positions 432, 434, or 435 were not activated by extracellular acidification and thus could not be assessed. The relative response to extracellular acidification after MTSET treatment was significantly different from controls in oocytes expressing A427C, G428C, L429C, and G431C channels (Fig. 2B).

Previous studies demonstrated that ENaCs with a Cys substitution at position 583 in the  $\alpha$  subunit or 536 in the  $\gamma$  subunit, homologous to ASIC1a 438, are irreversibly blocked by MTSET (16, 17). Our studies indicate that the Cys at position 438 is not accessible to MTSET, or alternatively, MTSET modification does not modify the response of the mutant channel to extracellular acidification (Fig. 2). To distinguish between these two possibilities, we investigated the effects of MTSEA on G438C channels at pH 7.4, *i.e.* channels in the resting state, and pH 6.5, *i.e.* channels in the open state (Fig. 3). Oocytes expressing C70L channels served as control in these studies. MTSEA is a membrane-permeable positively charged thiol-modifying reagent with a molecular diameter of  $\sim 3.6$  Å. MTSEA induces an increase in current in oocytes expressing G438C channels at both pH 7.4 and pH 6.5. The time course of change in current following MTSEA exposure was considerably faster at pH 6.5 than 7.4 (Fig. 3). The time constants ( $\tau$ ) of the current increase evoked by MTSEA at pH 6.5 and 7.4 were  $4.7 \pm 0.2$  s ( $n = 12$ ) and  $28.5 \pm 2.2$  s ( $n = 5$ ), respectively. This suggests that pore

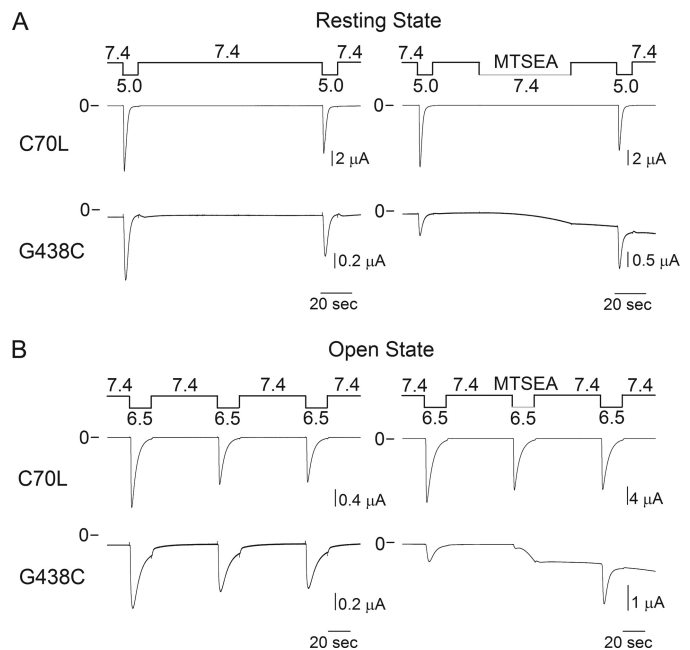


**FIGURE 3. G438C channels are covalently modified by MTSEA.** Representative recordings of proton-activated currents obtained from oocytes expressing controls (C70L) and G438C channels treated with MTSEA in the resting (pH 7.4) and conductive states (pH 6.5) are shown. ASIC1a mutants have a C-terminal HA epitope tag. Untreated oocytes expressing G438C and C70L channels served as controls ( $n = 5-11$ ).

opening facilitates the access of MTSEA to the target Cys (Fig. 3). At pH 7.4, the closed gate should prevent the permeation of MTSEA into the intracellular vestibule. Because MTSEA has a  $pK_a$  of 8.5 (25), at neutral pH, a fraction of unprotonated molecules could partition into the membrane environment. In this regard, previous studies indicated that intracellular residues of potassium channels are modified by external MTSEA in the closed state (26, 27). Our observed modification of G438C channels by MTSEA in the resting state (pH 7.4) suggests that this reagent gains access to the target Cys by passive diffusion through the lipid bilayer. In the conductive state, the limited reactivity of residues distal to Gly-431 toward MTSEA, but not MTSEA, denotes the presence of a molecular constraint that prevents the permeation of large cations from the extracellular vestibule into the ASIC1a pore.

**Ion Selectivity**—ASIC1a displays moderate selectivity for  $\text{Na}^+$  over  $\text{K}^+$  (2–5). To gain insight into the mechanism of ion selectivity of ASIC1a, we assessed the  $\text{K}^+/\text{Na}^+$  permeability of channels bearing single Cys substitutions in the TM2 segment (Fig. 4). In these studies, control (C70L) or mutant channels expressed in *X. laevis* oocytes were activated by a drop in extracellular pH from 8.0 to 5.0. The  $\text{K}^+/\text{Na}^+$  permeability was defined as the ratio of the peak current evoked by a drop in extracellular pH in a solution containing  $\text{K}^+$  as the main permeable cation to the peak current evoked by a drop in extracellular pH in a solution containing  $\text{Na}^+$  as the main permeable cation. The  $\text{K}^+/\text{Na}^+$  permeability for controls (C70L) was  $0.33 \pm 0.02$  ( $n = 13$ ) (Fig. 4), consistent with the  $\text{K}^+/\text{Na}^+$  permeability estimated from single channel studies on lamprey ASIC1 (IASIC1) ( $\text{K}^+/\text{Na}^+$  permeability 0.2) (5, 28). Substitutions at positions 431, 437, 438, 443, and 446 changed significantly the  $\text{K}^+/\text{Na}^+$  permeability of ASIC1a (Fig. 4A). Repetitive

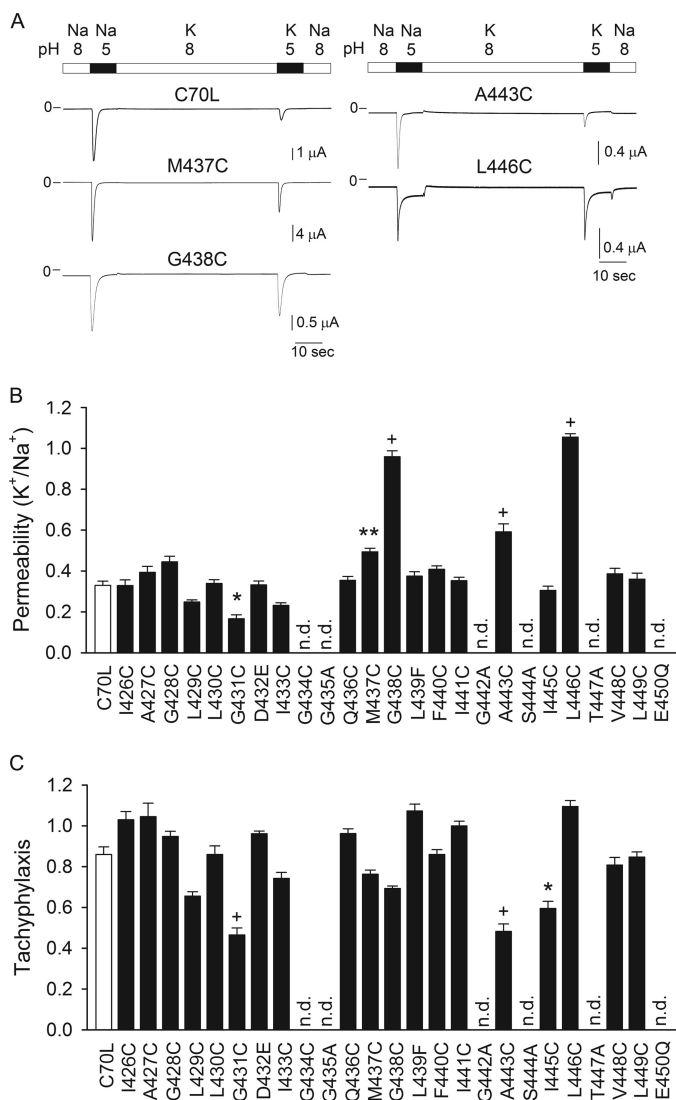


**FIGURE 4. Contribution of residues in TM2 segment to ion selectivity.** A, representative recordings of proton-activated currents obtained from oocytes expressing ASIC1a mutants. Whole-cell currents were elicited by a change in extracellular pH from 8.0 to 5.0 with Na<sup>+</sup> or K<sup>+</sup> as the main permeable cation. B, K<sup>+</sup>/Na<sup>+</sup> permeability of mutant ASIC1a channels. ASIC1a mutants have a C-terminal HA epitope tag. Whole-cell currents were elicited by a change in extracellular pH from 8.0 to 5.0. The peak current evoked by extracellular acidification with K<sup>+</sup> as the main permeable cation was normalized to the peak current evoked by extracellular acidification with Na<sup>+</sup> as the main permeable cation. Currents were normalized by tachyphylaxis (see below). C, tachyphylaxis of ASIC1a mutants. The response to repetitive acid stimulations was determined with Na<sup>+</sup> as the main permeable cation. ASIC1a mutants were activated by a change in extracellular pH from 8 to 5. Tachyphylaxis is defined as the ratio of the peak currents of two consecutive activations elicited by extracellular acidification (second peak current relative to the first peak current). Statistically significant differences with the control (C70L) are indicated as \*,  $p < 0.05$ , \*\*,  $p < 0.01$ , and +  $p < 0.001$  ( $n = 10-43$ ) (Kruskal-Wallis test followed by Dunn's multiple comparisons test). n.d., not detectable.

activation by extracellular acidification of some of the mutants assessed in this study resulted in constitutive desensitization to differing extents (Fig. 4B). Several Cys mutants were not activated by a drop in extracellular pH, and therefore, we generated additional substitutions at these sites (Fig. 4, B and C). G434C, G435C, G435A, L439C, G442C, G442A, S444C, S444A, T447C, T447A, E450C, and E450Q channels were not activated by extracellular acidification. Gly-442 and Ser-444 are located at

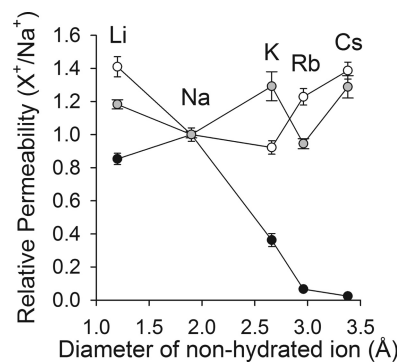


**FIGURE 5. Selectivity of ASIC1a mutants toward alkali metals.** The symbols represent relative permeability toward alkali metals of C70L channels (black circles), G438C (white circles), and G438A channels (gray circles). Whole-cell currents were elicited by a change in extracellular pH from 8.0 to 5.0 with solutions containing Na<sup>+</sup>, Li<sup>+</sup>, K<sup>+</sup>, Rb<sup>+</sup>, or Cs<sup>+</sup> as the main permeable cations. The peak current evoked by extracellular acidification with a defined alkali metal as the main permeable cation was normalized to the peak current evoked by extracellular acidification with Na<sup>+</sup> as the main permeable cation. The relative permeability (X<sup>+</sup>/Na<sup>+</sup>) is plotted as a function of the diameter of the nonhydrated cations ( $n = 8-15$ ).

sites analogous to the first and third residues in the conserved (G/S)XS tract of ENaC that contribute to its Na<sup>+</sup> selectivity (15, 17-19). ENaCs and ASICs bearing substitutions at these sites have reduced activity (15, 18, 19, 28).

ASIC1a is permeable to Na<sup>+</sup>, Li<sup>+</sup>, K<sup>+</sup> and Rb<sup>+</sup>, but virtually impermeable to Cs<sup>+</sup> (Fig. 5). Our results showed that substitutions at positions 431, 437, 438, 443 and 446 alter cation discrimination. It is broadly recognized that ion selectivity requires the interaction of ions with surface adsorption sites within the pore of the protein (11). To gain insight into the mechanism of ion selectivity of ASIC1a we investigated the permeability to alkali metals of M437C, G438C, G438A, A443C, and L446C channels (Fig. 5 and Table 1). The permeability (X<sup>+</sup>/Na<sup>+</sup>, where X<sup>+</sup> indicates Na<sup>+</sup>, Li<sup>+</sup>, K<sup>+</sup>, Rb<sup>+</sup>, or Cs<sup>+</sup>) was determined as the ratio of the peak currents evoked by extracellular acidification in a solution containing a defined alkali metal as the main permeable cation to the peak current evoked by extracellular acidification in a solution containing Na<sup>+</sup> as the main permeable cation. G438C and G438A were permeable to different extents to all alkali metals (Fig. 5 and Table 1). For both mutants, the permeability toward alkali metals was independent of the diameter of the nonhydrated ion. Substitutions at positions 437 and 443 increased the permeability to large cations, without altering the permeability to Li<sup>+</sup> (Table 1). L446C does not discriminate between Li<sup>+</sup>, Na<sup>+</sup>, K<sup>+</sup>, Rb<sup>+</sup>, and Cs<sup>+</sup>; essentially, ion discrimination is lost with this mutant. L446C does not desensitize completely; it remains partially open at pH 5.0, suggesting that this mutation also influences the mechanism of pore closing.

## DISCUSSION

To define structural rearrangements in the permeation pathway that occur during pore opening, we investigated the reactivity toward MTSET of channels bearing Cys mutations in the TM2 segment. MTSET treatment at pH 6.5 modifies the magnitude of the response to extracellular acidification of channels bearing Cys substitutions at positions 427, 428, 429, and 431. Our results indicate that MTSET is not able to permeate from

TABLE 1

## Relative permeability of ASIC1a mutants toward alkali metals

Whole-cell currents were elicited by a change in extracellular pH from 8.0 to 5.0. The peak current evoked by extracellular acidification with a defined alkali metal as the main permeable cation was normalized to the peak current evoked by extracellular acidification with Na<sup>+</sup> as the main permeable cation. Statistically significant differences with the control (C70L) are indicated as \*,  $p < 0.05$ , \*\*,  $p < 0.01$ , and \*\*\*,  $p < 0.001$  ( $n = 7-41$ ) (Kruskal-Wallis test followed by Dunn's multiple comparisons test).

	Li <sup>+</sup> /Na <sup>+</sup>	Na <sup>+</sup> /Na <sup>+</sup>	K <sup>+</sup> /Na <sup>+</sup>	Rb <sup>+</sup> /Na <sup>+</sup>	Cs <sup>+</sup> /Na <sup>+</sup>
C70L	0.85 ± 0.03	1.00 ± 0.04	0.33 ± 0.02	0.06 ± 0.01	0.02 ± 0.01
M437C	0.75 ± 0.05	1.00 ± 0.02	0.49 ± 0.02*	0.25 ± 0.03	0.20 ± 0.03
G438A	1.18 ± 0.03*	1.00 ± 0.02	1.29 ± 0.09***	0.94 ± 0.03***	1.29 ± 0.07***
G438C	1.40 ± 0.06***	1.00 ± 0.01	0.96 ± 0.03***	1.23 ± 0.05***	1.38 ± 0.05***
A443C	0.60 ± 0.04	1.00 ± 0.06	0.59 ± 0.04**	0.25 ± 0.03	0.25 ± 0.02
L446C	1.05 ± 0.03	1.00 ± 0.02	1.05 ± 0.02***	1.04 ± 0.04***	1.05 ± 0.04***

the extracellular to the intracellular vestibule of ASIC1a. We found that G438C channels were modified by MTSEA in the resting and open states, but not by MTSET (Fig. 3). The modification of G438C channels by MTSEA was faster at pH 6.5 than 7.4. We conclude that pore opening facilitates MTSEA access to the Cys at position 438. Interestingly, G438C channels were not able to return back to the resting state after MTSEA modification. The MTSEA-modified channels reside in a conductive state at pH 7.4. The differences in reactivity of G438C channels toward MTSEA and MTSET denote the presence of an element between residues 432 and 437 that restricts the diffusion of positively charged molecules based on its size. Substitutions at the homologous position of ASIC1a Gly-438 on the ENaC subunits significantly reduced the apparent affinity for amiloride (29). Moreover, channels bearing Cys mutations at these sites in the  $\alpha$  ( $\alpha$ S583C $\beta$  $\gamma$ ) and  $\gamma$  ( $\alpha$  $\beta$  $\gamma$ G542C) subunits are irreversibly blocked by MTSET (16, 17). Taken together, these results indicate subtle differences in the pore architecture of ASIC1a and ENaC. Our studies of accessibility with MTS reagents indicate that the permeation pathway in ASIC1a narrows in the open state below the gate (at Asp-433), restricting the passage of large molecules such as MTSET.

Here we explored the contribution of residues in the TM2 segment of ASIC1a to ion selectivity. ASIC1a shows a selectivity sequence toward alkali metal of Na<sup>+</sup> > Li<sup>+</sup> > K<sup>+</sup> >> Rb<sup>+</sup> > Cs<sup>+</sup>. The fact that Li<sup>+</sup> is less permeable than Na<sup>+</sup> suggests that permeation is not only a function of the diameter of the nonhydrated ion. Consequently, ion discrimination must necessarily be accomplished by coordination of ions to sites within the pore of the channel. Substitution of residues at positions 431, 437, 438, 443, and 446 changed the selectivity of ASIC1a toward alkali cations. Removal of the primary hydration shell and coordination by polar groups within the permeation pathway are considered the main determinants in ion selectivity (11). The selectivity sequence for alkali metals of ASIC1a is consistent with the Eisenman sequence for equilibrium ion exchange X (30). The energy of the interaction in an Eisenman model for an ion with ion-selective glasses is governed by the dehydration energies, the radius of the anionic binding site, and the cation radius. Eisenman sequence X illustrates a relatively strong interaction between the cation and the coordination site (11).

Channels bearing Cys and Ala substitutions at positions 438 discriminate poorly between alkali metals. G438C channels have a permeability sequence Li<sup>+</sup> ~ Cs<sup>+</sup> > Rb<sup>+</sup> > Na<sup>+</sup> ~ K<sup>+</sup>. This sequence does not conform to any of the 11 sequences predicted by Eisenman based on ion-selective electrodes (30). Lauser (31) developed a method based on rate theory to calcu-

late transport rates in ion channels using structural data, force constants, and intermolecular energy parameters, which predicted additional sequences for alkali metal cations. The model states that the selectivity of the channel depends on the rigidity of the coordination site, *i.e.* on the extent to which the interaction with the ion modifies the orientation of the coordination groups. Gly has a high conformational flexibility, which makes it particularly suitable to constitute an ion coordination site. The rates of desensitization and tachyphylaxis of G438C channels were similar to controls, suggesting that this mutation does not significantly alter channel gating. In addition, we found that mutations introduced at a neighboring position, Met-437, also changed the selectivity of the channel toward alkali metal cations. Our results are consistent with Gly-438 constituting a coordination site for alkali metals. It is possible that substitutions at this site or at other sites may indirectly affect ion binding by changing the orientation of neighboring coordination sites. Mutations introduced at the homologous position to Gly-438 on the ENaC subunits reduce the apparent affinity for amiloride (29), consistent with the predicted amiloride binding site at a depth of ~15% within the transmembrane electric field (32, 33). Na<sup>+</sup> and Li<sup>+</sup> compete with amiloride in the pore of ENaC, reducing the affinity for its binding site in a voltage-independent manner (34). Although K<sup>+</sup> itself acts as an ENaC blocker, it also competes with amiloride for the binding site, and this competition is strongly affected by the applied voltage (34). Substitutions at the amiloride binding site on the  $\beta$  and  $\gamma$  ENaC subunits reduced unitary conductance without changing the Li<sup>+</sup>/Na<sup>+</sup> selectivity of the channel (29, 35). These studies suggest that this site is important for ion coordination in other members of the family.

We identified additional sites in the TM2 segment where substitutions altered the selectivity of the channel toward alkali metals. Gly-431 is located in the outer vestibule of the pore in the desensitized state. Channels bearing Cys mutations at this position presented a lower K<sup>+</sup>/Na<sup>+</sup> selectivity than controls and enhanced tachyphylaxis. Bulky mutations at homologous sites to Gly-431 on ENaC/DEG channels increase dramatically the open probability (36-40). We hypothesize that the observed increased selectivity of G431C channels toward Na<sup>+</sup> is a consequence of a change in the structure of the  $\alpha$ -helix provoked by the mutation, but not a direct effect on ion coordination. Mutations at two additional sites reduced the selectivity of ASIC1a, position 443, in the (G/S)XS tract, and position 446, one helical turn below. The relative permeability to K<sup>+</sup>, Rb<sup>+</sup>, and Cs<sup>+</sup> was increased in A443C channels, consistent with Ala-443 being part of or near the putative selectivity filter.

The increased permeability of A443C to large alkali metals is consistent with previous studies suggesting that the (G/S)XS tract on ENaC acts as a molecular sieve (18). Unfortunately, we were unable to determine the selectivity of channels with mutations at the neighboring residues (442 and 444) as channels bearing mutations at these sites were not functional. We hypothesize that substitutions in all three subunits at position 443 may compromise the functionality of the (G/S)XS tract as a molecular sieve (18). Interestingly, concatemeric IASIC1 bearing a subunit with a Cys substitution at the first position of the (G/S)XS tract has a  $K^+/Na^+$  selectivity similar to wild type channels, but a reduced  $Li^+/Na^+$  permeability (28). A443C shows enhanced tachyphylaxis when compared with wild type channels, indicating that in addition to changing the selectivity toward alkali metals, this mutation also alters gating. L446C does not discriminate between the alkali metals that we tested. This mutant does not desensitize to the extent observed with wild type channels. Our results suggest that mutations at some sites modify selectivity and gating possibly by disturbing the structure of the pore-lining  $\alpha$ -helices. Examples of state-dependent changes in ion selectivity in ion channels have been previously reported (11). The C $\alpha$  atoms of Ala-443 and Leu-446 are positioned at 8.4 and 12.6 Å from the center of the pore in the desensitized state (PDB code: 3HGC), respectively (Fig. 1C). To contribute to ion selectivity, residues in the (G/S)XS tract must undergo a considerable movement toward the center of pore during opening. We have proposed that a rotation of the TM2 segments could widen the closed gate and move toward the center of the pore residues that contribute to ion selectivity in the distal region of the TM2 segments (24).

Our findings suggest that residues in an extended tract, from Met-437 through Leu-446, including the previously described (G/S)XS tract, contribute to discrimination of alkali metals on ASIC1a. We propose that cation selectivity is accomplished by the contribution of multiple sites in the inner pore of ASIC1a.

## REFERENCES

- Kellenberger, S., and Schild, L. (2002) Epithelial sodium channel/degenerin family of ion channels: a variety of functions for a shared structure. *Physiol. Rev.* **82**, 735–767
- Meltzer, R. H., Kapoor, N., Qadri, Y. J., Anderson, S. J., Fuller, C. M., and Benos, D. J. (2007) Heteromeric assembly of acid-sensitive ion channel and epithelial sodium channel subunits. *J. Biol. Chem.* **282**, 25548–25559
- Bässler, E. L., Ngo-Anh, T. J., Geisler, H. S., Ruppertsberg, J. P., and Gründer, S. (2001) Molecular and functional characterization of acid-sensing ion channel (ASIC) 1b. *J. Biol. Chem.* **276**, 33782–33787
- Waldmann, R., Champigny, G., Bassilana, F., Heurteaux, C., and Lazdunski, M. (1997) A proton-gated cation channel involved in acid sensing. *Nature* **386**, 173–177
- Li, T., Yang, Y., and Canessa, C. M. (2011) Asp-433 in the closing gate of ASIC1 determines stability of the open state without changing properties of the selectivity filter or  $Ca^{2+}$  block. *J. Gen. Physiol.* **137**, 289–297
- Wemmie, J. A., Chen, J., Askwith, C. C., Hruska-Hageman, A. M., Price, M. P., Nolan, B. C., Yoder, P. G., Lamani, E., Hoshi, T., Freeman, J. H., Jr., and Welsh, M. J. (2002) The acid-activated ion channel ASIC contributes to synaptic plasticity, learning, and memory. *Neuron* **34**, 463–477
- Deval, E., Gasull, X., Noël, J., Salinas, M., Baron, A., Diochot, S., and Lingueglia, E. (2010) Acid-sensing ion channels (ASICs): pharmacology and implication in pain. *Pharmacol Ther* **128**, 549–558
- Wemmie, J. A., Price, M. P., and Welsh, M. J. (2006) Acid-sensing ion channels: advances, questions, and therapeutic opportunities. *Trends Neurosci* **29**, 578–586
- Garty, H., and Benos, D. J. (1988) Characteristics and regulatory mechanisms of the amiloride-blockable  $Na^+$  channel. *Physiol. Rev.* **68**, 309–373
- Garty, H., and Palmer, L. G. (1997) Epithelial sodium channels: function, structure, and regulation. *Physiol. Rev.* **77**, 359–396
- Hille, B. (2001) *Ionic Channels of Excitable Membranes*, Third Ed., Sinauer Associates Inc., Sunderland, MA
- Derebe, M. G., Sauer, D. B., Zeng, W., Alam, A., Shi, N., and Jiang, Y. (2011) Tuning the ion selectivity of tetrameric cation channels by changing the number of ion binding sites. *Proc. Natl. Acad. Sci. U.S.A.* **108**, 598–602
- Gonzales, E. B., Kawate, T., and Gouaux, E. (2009) Pore architecture and ion sites in acid-sensing ion channels and P2X receptors. *Nature* **460**, 599–604
- Kashlan, O. B., Sheng, S., and Kleyman, T. R. (2005) On the interaction between amiloride and its putative  $\alpha$ -subunit epithelial  $Na^+$  channel binding site. *J. Biol. Chem.* **280**, 26206–26215
- Sheng, S., Li, J., McNulty, K. A., Avery, D., and Kleyman, T. R. (2000) Characterization of the selectivity filter of the epithelial sodium channel. *J. Biol. Chem.* **275**, 8572–8581
- Sheng, S., Li, J., McNulty, K. A., Kieber-Emmons, T., and Kleyman, T. R. (2001) Epithelial sodium channel pore region: structure and role in gating. *J. Biol. Chem.* **276**, 1326–1334
- Snyder, P. M., Olson, D. R., and Bucher, D. B. (1999) A pore segment in DEG/ENaC  $Na^+$  channels. *J. Biol. Chem.* **274**, 28484–28490
- Kellenberger, S., Gautschi, I., and Schild, L. (1999) A single point mutation in the pore region of the epithelial  $Na^+$  channel changes ion selectivity by modifying molecular sieving. *Proc. Natl. Acad. Sci. U.S.A.* **96**, 4170–4175
- Kellenberger, S., Hoffmann-Pochon, N., Gautschi, I., Schneeberger, E., and Schild, L. (1999) On the molecular basis of ion permeation in the epithelial  $Na^+$  channel. *J. Gen. Physiol.* **114**, 13–30
- Kellenberger, S., Auberson, M., Gautschi, I., Schneeberger, E., and Schild, L. (2001) Permeability properties of ENaC selectivity filter mutants. *J. Gen. Physiol.* **118**, 679–692
- Passero, C. J., Okumura, S., and Carattino, M. D. (2009) Conformational changes associated with proton-dependent gating of ASIC1a. *J. Biol. Chem.* **284**, 36473–36481
- Chen, X., and Gründer, S. (2007) Permeating protons contribute to tachyphylaxis of the acid-sensing ion channel (ASIC) 1a. *J. Physiol.* **579**, 657–670
- Jasti, J., Furukawa, H., Gonzales, E. B., and Gouaux, E. (2007) Structure of acid-sensing ion channel 1 at 1.9 Å resolution and low pH. *Nature* **449**, 316–323
- Tolino, L. A., Okumura, S., Kashlan, O. B., and Carattino, M. D. (2011) Insights into the mechanism of pore opening of acid-sensing ion channel 1a. *J. Biol. Chem.* **286**, 16297–16307
- Karlin, A., and Akabas, M. H. (1998) Substituted-cysteine accessibility method. *Methods Enzymol.* **293**, 123–145
- Holmgren, M., Liu, Y., Xu, Y., and Yellen, G. (1996) On the use of thiol-modifying agents to determine channel topology. *Neuropharmacology* **35**, 797–804
- Zhang, Y. Y., Sackin, H., and Palmer, L. G. (2006) Localization of the pH gate in Kir1.1 channels. *Biophys. J.* **91**, 2901–2909
- Li, T., Yang, Y., and Canessa, C. M. (2011) Outlines of the pore in open and closed conformations describe the gating mechanism of ASIC1. *Nat. Commun.* **2**, 399
- Schild, L., Schneeberger, E., Gautschi, I., and Firsov, D. (1997) Identification of amino acid residues in the  $\alpha$ ,  $\beta$ , and  $\gamma$  subunits of the epithelial sodium channel (ENaC) involved in amiloride block and ion permeation. *J. Gen. Physiol.* **109**, 15–26
- Eisenman, G. (1962) Cation-selective glass electrodes and their mode of operation. *Biophys. J.* **2**, 259–323
- Läuger, P. (1982) Microscopic calculation of ion-transport rates in membrane channels. *Biophys. Chem.* **15**, 89–100
- Palmer, L. G. (1984) Voltage-dependent block by amiloride and other monovalent cations of apical Na channels in the toad urinary bladder. *J. Membr. Biol.* **80**, 153–165
- Palmer, L. G. (1985) Interactions of amiloride and other blocking cations with the apical Na channel in the toad urinary bladder. *J. Membr. Biol.* **87**, 191–199

## ASIC1a Permeation Pathway

34. Palmer, L. G., and Andersen, O. S. (1989) Interactions of amiloride and small monovalent cations with the epithelial sodium channel: inferences about the nature of the channel pore. *Biophys. J.* **55**, 779–787
35. Li, J., Sheng, S., Perry, C. J., and Kleyman, T. R. (2003) Asymmetric organization of the pore region of the epithelial sodium channel. *J. Biol. Chem.* **278**, 13867–13874
36. Carattino, M. D., Sheng, S., and Kleyman, T. R. (2004) Epithelial Na<sup>+</sup> channels are activated by laminar shear stress. *J. Biol. Chem.* **279**, 4120–4126
37. Snyder, P. M., Bucher, D. B., and Olson, D. R. (2000) Gating induces a conformational change in the outer vestibule of ENaC. *J. Gen. Physiol.* **116**, 781–790
38. Pfister, Y., Gautschi, I., Takeda, A. N., van Bemmelen, M., Kellenberger, S., and Schild, L. (2006) A gating mutation in the internal pore of ASIC1a. *J. Biol. Chem.* **281**, 11787–11791
39. Brown, A. L., Fernandez-Illescas, S. M., Liao, Z., and Goodman, M. B. (2007) Gain-of-function mutations in the MEC-4 DEG/ENaC sensory mechanotransduction channel alter gating and drug blockade. *J. Gen. Physiol.* **129**, 161–173
40. Kellenberger, S., Gautschi, I., and Schild, L. (2002) An external site controls closing of the epithelial Na<sup>+</sup> channel ENaC. *J. Physiol.* **543**, 413–424